Control of Electrochemical and Ferryloxy Formation Kinetics of Cyt P450s in Polyion Films by Heme Iron Spin State and Secondary Structure

Sadagopan Krishnan, Amila Abeykoon, John B Schenkman, and James F Rusling

SUPPORTING INFORMATION

Experimental, additional details

Film assembly. Polyion and enzyme films were assembled layer-by-layer on basal plane pyrolytic graphite (PG) electrodes similar to our previous reports. [1,2,3] Prior to the film assembly, PG electrodes were abraded on 400-grit SiC paper (Buehler), then roughened on medium Crystal Bay emery paper (PH 3M 001K), and then ultrasonicated in ethanol for 30 s followed by in water for 30 s, and finally dried in a stream of nitrogen. The following solutions were used to construct the layer-by-layer films: (a) 3 mg mL^{-1} PSS plus 0.5 M NaCl in deionized water; (b) 1 mg mL^{-1} PEI or PDDA plus 0.05 M NaCl in deionized water; (c) 1 mg mL^{-1} cyt P450s and catalase solutions prepared in 50 mM phosphate buffer, pH 7.0; (d) 1 mg mL^{-1} myoglobin made in 10 mM sodium acetate buffer, pH 4.5; (e) 1 mg mL^{-1} hemin solution prepared in 50 mM sodium carbonate buffer, pH 10. Assemblies of PEI(/PSS/enzyme)$_4$ [where enzyme = P450 1A2 or 2E1 or myoglobin] were made on PG electrodes. Here the polycation (PEI) is adsorbed as first layer on the roughened PG electrode surface followed by alternate adsorption cycles of polyanion (PSS) and the positively charged enzyme with one layer at a time. The electrodes were rinsed in water between each layer adsorption to remove weakly bound molecules.

The initial PEI and PSS layers were adsorbed for 20 min. at room temperature followed by the enzyme and subsequent layers adsorbed for 30 min. at 4^{o}C to give the stable and reproducible film assembly known from the QCM sensors. Similarly PSS(/PEI/enzyme)$_4$ [where enzyme = P450cam or catalase, or hemin films in place of enzyme] films were assembled for these negatively charged enzymes.

Spectra were obtained with films fabricated on aminosilane-derivatized fused silica slides. Difference spectra of Fe^{II}-CO protein complexes were obtained by first reducing ferric cyt P450 to ferrous using sodium dithionite (10 mM) in 50 mM phosphate buffer, pH 7.0. The buffer was then purged with CO and the spectrum was acquired against the cyt P450 film that was reduced with dithionite, but had no CO.

The representations in Figure 9 were created using the program Maestro 8.5, Schrodinger LLC, NY 2008.

Simulation of thin-film voltammograms. All the simulations were performed using CHI Instruments digital simulation software. For the simulation of direct electron transfer kinetics, we used surface confined Butler-Volmer models and compared our simulated peak separations and oxidation and reduction peaks potentials with the experimental data to obtain the best fit.

The specific mechanisms used for the simulations were E reduction/E oxidation and EC reduction/E oxidation, where E = electron transfer, and C = chemical reaction. Common conditions used for both simulation mechanisms were: surface confined process (i.e. thin film voltammetry); potential range and scan rates the same as in experimental CVs; experimentally determined electroactive amount of the enzymes was used; electrode area = 0.2 cm^2; capacitance = 5 μF; temperature = 25 ^{o}C.

The pathway and the best fit simulation parameters used for the **E reduction/E oxidation** mechanism are as follows"

$$A + e \rightarrow B \text{ -------- (1) } k_{s,red} = 18\ s^{-1};\ Eo = -0.338\ V;\ \alpha = 0.5$$
$$B' - e \rightarrow C \text{ -------- (2) } k_{s,red} = 18000\ s^{-1};\ Eo = -0.330\ V;\ \alpha = 0.5$$

The simulations were done over the scan rate range 0.005 to 1.4 V s^{-1} as used for experiments. To compare the simulation trend with the experimental trumpet plots of all the protein films, the Ep,red and Ep,ox values obtained from simulation were adjusted with appropriate magnitudes of potential to match the starting experimental peak potential values in the trumpet plots (Figure 6). This compensation in simulated peak potentials did not affect the values of peak separation with increasing scan rates and the simulation trend, but positioned simulation data in line with the experimental trumpet plot points for comparison. Representative CVs obtained from E reduction/E oxidation simulation of cyt P450 2E1 films is shown in Figure S7.

For the **EC reduction/E oxidation** simulation, parameters and pathway was as follows:

$$A + e \rightarrow B \text{ -------- (1) } k_{s,red} = 18\ s^{-1};\ Eo = -0.338\ V;\ \alpha = 0.5$$
$$B \leftrightarrow C \text{ -------- (3) } \quad k_f = 3.6\ s^{-1};\ k_b = 0.018\ s^{-1}$$
$$C - e \rightarrow D \text{ -------- (4) } \quad k_{s,ox} = 18000\ s^{-1};\ Eo = -0.330\ V;\ \alpha = 0.5$$

Here eqs. (1) and (4) are the electrochemical reduction and oxidation steps. And eq.(3) corresponds to the chemical equilibrium following the reduction. The above parameters gave us the best fit that had similar experimental trumpet plot trend, however the shifts in $E_{p,red}$ with increasing scan rates were smaller than the experimental one (see Figure S8).

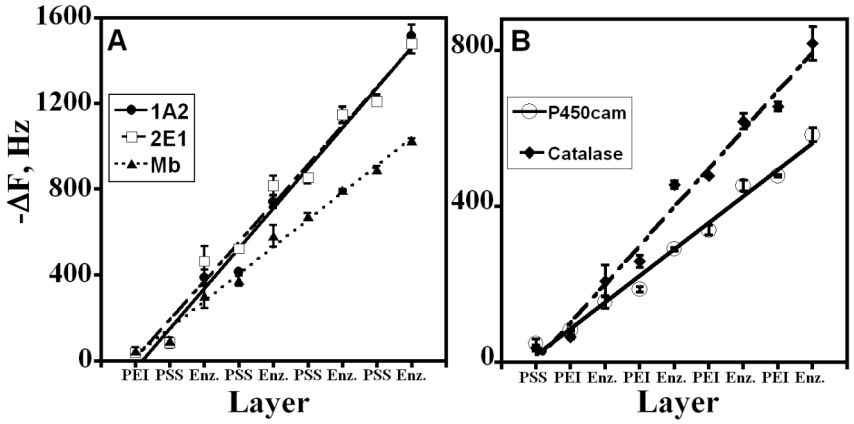

Figure S1. QCM frequency shifts for cycles of alternate (A) PSS/ enzyme (P450 1A2 or 2E1 or Mb) and (B)PEI/enzyme (P450cam or catalase) adsorption on gold resonators coated with a monolayer of 3-mercaptopropionic acid as first layer and PEI (A) / PSS (B) as second layer.

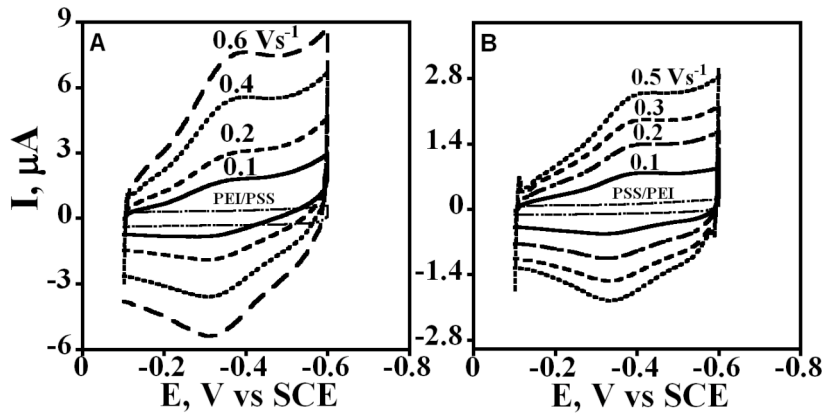

Figure S2. Cyclic voltammograms without background subtraction of (A) PEI(/PSS/P450 2E1)$_4$ and (B) PSS(/PEI/P450cam)$_4$ films on pyrolytic graphite electrodes with increasing scan rates in anaerobic 50 mM potassium phosphate buffer + 0.1 M NaCl, pH 7.0 .

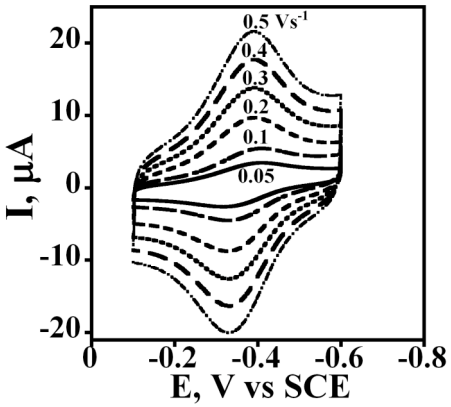

Figure S3. Cyclic voltammograms of PSS(/PEI/hemin)$_4$ films on pyrolytic graphite electrodes with increasing scan rates in anaerobic 50 mM potassium phosphate buffer + 0.1 M NaCl, pH 7.0 .

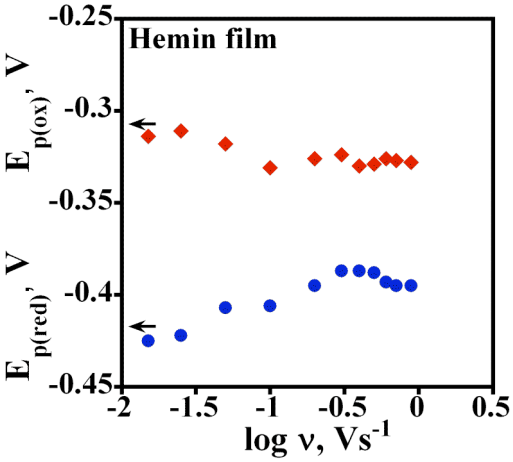

Figure S4. Influence of increasing cyclic voltammetry scan rates on experimental peak separation (ΔE_p) for PSS(/PEI/hemin)$_4$ films on PG electrodes in anaerobic 50 mM potassium phosphate buffer + 0.1 M NaCl, pH 7.0 .

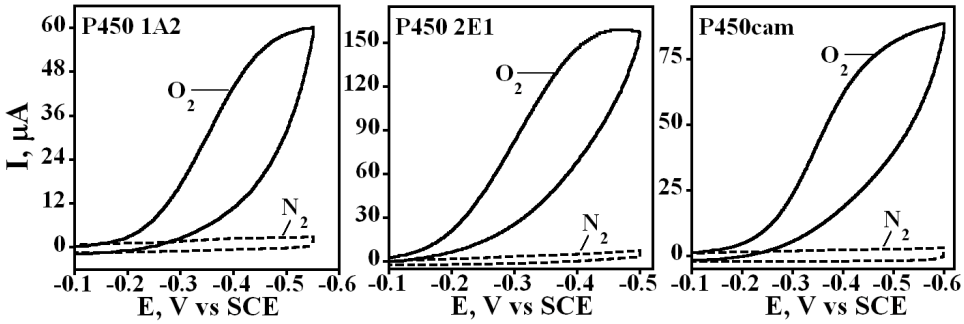

Figure S5. Cyclic voltammograms at 0.1 Vs^{-1} in 50 mM potassium phosphate, pH 7.0 buffer + 0.1 M NaCl, in a sealed cell for polyion/P450 enzyme films on PG electrodes in nitrogen and in buffer saturated with oxygen. In the presence of oxygen, P450 Fe(II)/O_2 complex is formed after P450 Fe(III) is reduced on the electrode. Electrochemical reduction of this P450 Fe(II)/O_2 complex gives hydrogen peroxide at the Fe(III)/Fe(II) redox potential. This catalytic reduction can be detected by CV as an increase in reduction peak current in the presence of oxygen with the disappearance of the oxidation peak for P450 Fe(II), consistent with its fast reaction with oxygen.

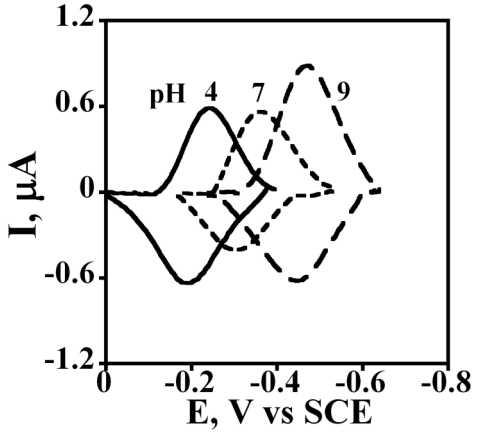

Figure S6. Background subtracted cyclic voltammograms at 0.1 Vs^{-1} for PEI(/PSS/P450 2E1)$_4$ film on PG electrodes at different pH values in anaerobic buffers containing 0.1 M NaCl. Positive shifts in formal potentials with lowering pH shows the proton coupled electron transfer in P450 enzyme films.

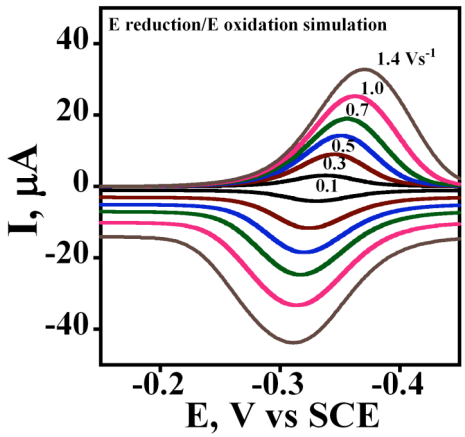

Figure S7. Digitally simulated CVs of cyt P450 2E1 films with increasing scan rates using E reduction/E oxidation mechanism. The trumpet plot lines of this simulation data is shown in Figure 6B.

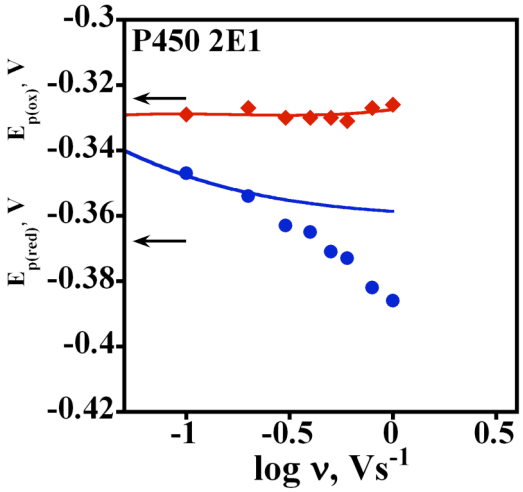

Figure S8. Oxidation (red diamonds) and reduction (blue circles) peak potentials vs. logarithm of scan rate for PEI(/PSS/P450 2E1)$_4$ films (experimental data as in Figure 6B). The lines represent the simulation results obtained using the EC reduction/E oxidation mechanism using the following electrochemical and chemical rate constants: $k_{s,red} = 18\ s^{-1}$; $k_{s,ox} = 18000\ s^{-1}$; $k_f = 3.6\ s^{-1}$; $k_b = 0.018\ s^{-1}$.

References

(1) (a) Rusling, J. F.; Hvastkovs, E. G.; Hull, D. O.; Schenkman, J. B. *Chem. Commun.* **2008**, 141 – 154; (b) Rusling, J. F.; Lvov, Y.; Mohwald, H. *Eds*., In *Protein Architecture: Interfacing Molecular Assemblies and Immobilization Biotechnology*, Marcel Dekker: New York, **2000**, 337-354.

(2) Zhou, L. ; Yang, Y.; Estavillo, C.; Stuart, J. D.; Schenkman, J. B.; Rusling, J. F. *J. Am.Chem. Soc.* **2003**, *125*, 1431-1436.

(3) (a) Zu, X.; Lu, Z.; Zhang, Z.; Schenkman, J. B.; Rusling, J. F. *Langmuir* **1999**, *15*, 7372-7377; (b) Munge, B.; Estavillo, C.; Schenkman, J. B.; Rusling, J. F. *ChemBioChem* **2003**, *4*, 82-89; (c) Estavillo, C.; Lu, Z.; Jansson, I.; Schenkman, J. B.; Rusling, J. F. *Biophys. Chem*. **2003**, *104*, 291-296.